2024 American Control Conference (ACC)
July 8-12, 2024. Toronto, Canada

Predator-Swarm-Guide Dynamics: A Hybrid Approach to Crowd Modeling and Guidance in Mass Shooting Scenarios

Atefe Darabi*, Hamidreza Montazeri Hedesh*, Milad Siami*, Mario Sznaier*

***Abstract*— This paper introduces the "Predator-Swarm-Guide" (PSG) model, a hybrid approach for modeling crowd dynamics by considering pairwise repulsive and attractive interactions among individuals. Extending the predator-swarm model, PSG specifically addresses the behavior of individuals during a shooting event within a zoned environment. It accounts for individuals' simultaneous efforts to evade the shooter while seeking guidance from a trusted agent. The guiding agent's movements during evacuation are influenced by two factors: its orientation towards the safe zone, where individuals are protected from the shooter, and the shooter's location. The PSG model incorporates crucial environmental factors, including impermeable walls, psychological elements leading to significant social friction, and a termination procedure to track casualties. Outputs of the PSG model underscore the significance of coordinated cooperation between individuals and the guiding agent in minimizing casualties during an active shooting scenario. Therefore, the objective is to reduce casualties through a hybrid motion optimization approach for both individuals and the guiding agent. Additionally, an equilibrium analysis, based on the continuum-limit version of the PSG model, is conducted to predict the crowd's equilibrium configuration in specific scenarios.**

I. Introduction

Crowd-related disasters, such as the Hillsborough disaster in 1989, the Hajj stampede in 2015, the Love Parade disaster in 2010, the 2022 Seoul Halloween crush, and the Astroworld Festival in 2021 [1]–[4], highlight the pressing need for effective crowd management strategies. The surge in active shooting events worldwide further underscores the urgency in developing swift and secure evacuation strategies. According to the Gun Violence Archive, the number of mass shootings in the United States alone was 383 in 2016, 415 in 2019, and 646 in 2022 [5]. These statistics underline the essential need for effective crowd modeling during emergencies to ensure the safety of civilians.

Crowd movement models broadly fall into microscopic and macroscopic categories [6]. Microscopic models consider individual behavior, accounting for factors like psychology, density, and environmental boundaries [7]. While precise, they can be computationally demanding for large crowds. On the other hand, macroscopic models, examining collective behavior, form the foundation of many crowd models [8]–[10].

Research in this area has focused on refining these models by incorporating psychological factors, social bonds, and herding instincts to enhance the realism of the current models [11]–[15]. Moreover, some studies have expanded their crowd models to include new roles. For instance, the behavior of a swarm of prey in the presence of a predator has been investigated in [16]. Additionally, some studies take into account the effect of control agents in crowd dynamics models, aiming to optimally guide the crowd towards a desired direction or destination [17], [18].

Drawing inspiration from the minimal microscopic model introduced in [16], our research presents a dynamic model specifically designed for active shooting events. The proposed model, called Predator-Swarm-Guide (PSG), incorporates novel elements such as a guiding agent, wall impermeability, and zoned environments to accurately capture the dynamics of such scenarios. PSG is a first-order model, offering enhanced analyzability and enabling the study of large crowd sizes, which is particularly useful for analyzing the escape scenarios within large venues, such as stadiums. By analyzing the impact of individual behaviors within the model, we can gain valuable insights into the overall outcomes of escape scenarios during active shooting events.

The paper proceeds as follows: Section II defines the simulation environment and introduces PSG. It outlines a termination procedure for affected individuals and explores individual behaviors' impact on escape outcomes. Section III formulates a multi-variable optimization problem to minimize casualties by adapting guidance routes and mass behavior. Equilibrium analysis investigating crowd configuration in the steady state is conducted in section IV. Section V presents our conclusions and final remarks.

II. Modified Predator-Swarm Interactions with a Guiding Agent

In this section, a modified model of predator-swarm interactions is introduced to investigate the outcomes of a shooting scenario under certain conditions. We consider a shooter as the predator, a guiding agent, and a group of individuals as the prey. The crowd-shooter and guide-crowd interactions are modeled considering the repulsion and attraction forces between them. Interactions are assumed to occur within a confined environment $\mathcal{R} \in [0,5]^2$. This room is bounded by walls described by line segments: w_1 (bottom) spanning $(0,0)$ to $(5,0)$, w_2 (right) from $(5,0)$ to $(5,5)$, w_3 (top) from

This material is based upon work supported in by grants ONR N00014-21-1-2431, NSF 2121121, NSF 2208182, the U.S. Department of Homeland Security under Grant Award Number 22STESE00001-03-02, and by the Army Research Laboratory under Cooperative Agreement Number W911NF-22-2-0001. The views and conclusions contained in this document are solely those of the authors and should not be interpreted as representing the official policies, either expressed or implied, of the U.S. Department of Homeland Security, the Army Research Office, or the U.S. Government.

*Department of Electrical & Computer Engineering, Northeastern University, Boston, MA 02115 USA (e-mails: {darabi.a, montazerihedesh.h, m.siami, m.sznaier}@northeastern.edu).

$(5,5)$ to $(0,5)$, and w_4 (left) from $(0,5)$ to $(0,0)$. These walls are collectively represented as $W = \{w_1, w_2, w_3, w_4\}$, distinctly separating $\mathcal{R}$ from external spaces. Within $\mathcal{R}$, we identify a safe zone $Z_s = [2.5, 5]^2$, a danger zone $Z_d = [0, 2.5]^2$, and two free zones, accessible to all. We assume that the shooter is restricted to moving within the danger and free zones and will be captured upon reaching the boundaries of the safe zone. The danger zone is the initial location of the crowd, making it the primary target of the shooter's actions. It is worth noting that our assumptions on the walls' coordinates are for illustration and clarity, and the results we derive can be extended to any set of walls.

The following subsection outlines the dynamics of a mass shooting event within the aforementioned environment.

A. Predator-Swarm-Guide Model

The modified predator-swarm model, referred to as the Predator-Swarm-Guide model in this study, is based on the dynamics established in [16]. However, new elements and notions are incorporated to adapt this model specifically for a mass shooting scenario. Assuming that the individuals in the crowd aim to follow the guiding agent while simultaneously avoiding the shooter and preventing collisions with other individuals, we next describe the PSG model.

We denote the position of the shooter, the guiding agent, and the j-th individual by $\mathbf{z}(t) \in \mathcal{R}$, $\mathbf{y}(t) \in \mathcal{R}$, and $\mathbf{x}_j(t) \in \mathcal{R}$ for $j \in \mathcal{V} = \{1, 2, \cdots, N\}$, respectively. To maintain brevity, we use the notations $\mathbf{z}$, $\mathbf{y}$, and $\mathbf{x}$ to represent the states $\mathbf{z}(t)$, $\mathbf{y}(t)$, and $\mathbf{x}(t)$ respectively throughout this paper.

We consider pair-wise attractive and repulsive forces to describe the interactions between individual j and the rest of the crowd. In this regard, the total force enacting on individual j is expressed by $\mathbf{F}_{j,II} = \frac{1}{N}\sum_{k=1,k\neq j}^{N} \frac{\mathbf{x}_j - \mathbf{x}_k}{|\mathbf{x}_j - \mathbf{x}_k|^2} - \alpha_1(\mathbf{x}_j - \mathbf{x}_k)$. The first term represents the inherent psychological inclination of individuals in close proximity to maintain distance from each other, enacted through a short-range repulsive force. The second term represents a linear long-range force between individuals. When individuals tend to emulate mass behaviors by following each other, an attractive interaction among them is generated which is denoted by $\alpha_1 > 0$. Conversely, when individuals aim to avoid each other to prevent congestion, a repulsive interaction is generated with a negative α_1 value.

The individuals in the distance are normally unable to see each other, and therefore, there is no interaction between them. We employ a decaying effect, as suggested by [19], to incorporate the effect of a reduced sightline, ensuring the force remains bounded. Incorporating the decaying effect involves modifying the linear force term $\alpha_1(\mathbf{x}_j - \mathbf{x}_k)$ by multiplying it with a decaying function $h(|\mathbf{x}_j - \mathbf{x}_k|)$. This function is defined as $h(r) = e^{r_0 - r}$ if $r > r_0$, and $h(r) = 1$ otherwise. In this context, $r = |\mathbf{x}_j - \mathbf{x}_k|$ represents the distance between two individuals j and k, and r_0 denotes a cutoff distance. When the distance is within the cutoff range ($r \leq r_0$), the function $h(r)$ takes the value of 1, implying no modification to the linear force. However, for distances beyond the cutoff range ($r > r_0$), the sightline is reduced, and the function decays exponentially, allowing the force to diminish as the distance increases.

As the individuals attempt to flee from the shooter, a repulsive effect is induced within the crowd against the shooter's presence. To model this effect, the j-th individual will exert a force away from the shooter given by $\mathbf{F}_{j,IS} = \alpha_2 \frac{\mathbf{x}_j - \mathbf{z}}{|\mathbf{x}_j - \mathbf{z}|^2}$. Here, α_2 represents the strength of the repulsive interaction between the individuals and the shooter.

To account for the impact of the agent's guidance on the j-th individual, we introduce an external attraction force denoted as $\mathbf{F}_{j,IA} = \alpha_3(\mathbf{x}_j - \mathbf{y})$. The parameter α_3 dictates the strength of attraction towards the guiding agent and reflects the level of trust that individuals have in the guidance provided. We assume that during a shooting event, all individuals are aware of the danger and actively strive to pay attention to the guiding agent and its location. In this scenario, individuals located farther from the guiding agent will exert more effort to approach and stay close to the guiding agent. It is important to note that since the simulations in this study are conducted in a confined room with boundaries, the influence of this force remains limited.

The shooter's objective is to pursue and target individuals who are in close proximity. Conversely, as individuals distance themselves from the shooter, the attractive force they exert on the shooter decreases. This force is denoted as $\mathbf{F}_S = \frac{\alpha_4}{N}\sum_{k=1}^{N} \frac{\mathbf{x}_k - \mathbf{z}}{|\mathbf{x}_k - \mathbf{z}|^p}$ and represents the average interaction between the shooter and the crowd. Each interaction follows a power law with exponent p, causing the interaction strength to decrease as the distance between the shooter ($\mathbf{z}$) and each member of the crowd ($\mathbf{x}_k$) increases. The parameter α_4 governs the strength of the shooter's attraction toward the crowd. We make the assumption that the shooter's movement is constrained to the danger and free zones within the room and that the shooter lacks prior information about the location of the safe zone. In the event that the shooter pursues the crowd and reaches the boundaries of the safe zone, the shooter is considered captured and the simulation is concluded.

The main objective of the guiding agent is to safely navigate the individuals from the danger zone to the designated safe zone while minimizing their exposure to the shooter. To achieve this objective, we first introduce a weighting parameter denoted as $0 \leq \lambda \leq 1$. This parameter dictates the priority of moving towards the safe target as opposed to moving away from the shooter. A value of λ closer to 1 emphasizes movement toward the target, while a value closer to 0 prioritizes moving away from the shooter. We express this weighted combination by

$$\mathbf{F}_A = \alpha_5 \lambda \frac{\mathbf{y}_r - \mathbf{y}}{|\mathbf{y}_r - \mathbf{y}|} + \alpha_5(1-\lambda)\frac{\bar{\mathbf{x}} - \mathbf{z}}{|\bar{\mathbf{x}} - \mathbf{z}|}, \tag{1}$$

where α_5 indicates the attraction level of the guiding agent toward the crowd. $\mathbf{y}_r$ represents the position of the guiding agent's target within the safe zone. $\bar{\mathbf{x}}$ denotes the average position of the crowd. Defining the dynamics of the guiding agent in this approach ensures that the guiding agent makes informed decisions to steer the individuals toward safety

while taking into account the presence of the shooter.

The impermeability of the walls can be incorporated by considering a repulsive effect on the individuals [20], [21] once they are located within the wall interaction range. Based on the approach outlined in [21], we introduce the total wall repulsive force acting on an individual with position $\mathbf{p} \in \{\mathbf{x}, \mathbf{z}, \mathbf{y}\}$ as $\mathbf{F}_W = \sum_{w_i \in W} \alpha_6 \left[\frac{1}{\mathrm{d}(w_i, \mathbf{p})} - \frac{1}{r_w}\right]_+ \mathbf{n}(w_i)$. The parameter α_6 represents the strength of repulsion against walls, $\mathrm{d}(w_i, \mathbf{p})$ denotes the distance between the individual and wall w_i, r_w is the interaction range of walls, and $\mathbf{n}(w_i)$ represents the outward unit normal vector of wall w_i. The operator $[X]_+$ returns the value X if $X > 0$ and returns zero otherwise. Note that the subscript $\{W\}$ in $\mathbf{F}_W$ will be replaced by $\{j, IW\}$ for individual j, by $\{SW\}$ for the shooter, and by $\{AW\}$ for the guiding agent.

While attempting to escape from the shooter, individuals seek safety by staying as close to the guiding agent as possible. In their effort to closely follow the agent, they experience increased "social friction", which can have a significant impact on their movement. Following the principles of Newtonian mechanics, the motion of each individual, denoted as i, with position $\mathbf{p} \in \{\mathbf{x}, \mathbf{z}, \mathbf{y}\}$, mass m_i, social friction coefficient μ_i, and the total force acting on them, denoted as $\mathbf{F}_i$, can be described by the equation $m_i \frac{d^2\mathbf{p}}{dt^2} + \mu_i \frac{d\mathbf{p}}{dt} = \mathbf{F}_i$. We assume that in mass shooting scenarios, the effect of social friction is significantly higher than the individual's mass, i.e., m_i is negligible compared to μ_i, and rescale the dynamics accordingly. This leads to simplified first-order dynamics for each individual.

We now proceed to present the first-order dynamics that describe an active shooting event, taking into account the interactions between the shooter, individuals, and the guiding agent.

$$\frac{d\mathbf{x}_j}{dt} = \mathbf{F}_{j,II} + \mathbf{F}_{j,IS} + \mathbf{F}_{j,IA} + \mathbf{F}_{j,IW}, \tag{2}$$

$$\frac{d\mathbf{z}}{dt} = \mathbf{F}_S + \mathbf{F}_{SW}, \tag{3}$$

$$\frac{d\mathbf{y}}{dt} = \mathbf{F}_A + \mathbf{F}_{AW}. \tag{4}$$

Note that in the model above, the friction (damping) force is equal to the net external force applied to each individual. For subsequent analysis in the upcoming sections, we employ the fourth-order Runge-Kutta method with a time step of $dt = 0.05$ to discretize the continuous dynamics outlined by equations (2), (3), and (4). In the model presented above, the removal of an individual from the system upon being attacked by the shooter is not explicitly considered. However, acknowledging the significance of this effect, we will address the termination procedure in the following subsection.

B. Termination Procedure

In the simulation of shooter-crowd interactions, the termination procedure plays a vital role in modeling the shooter's ability to target and eliminate members of the crowd. To implement this, we define a shot radius denoted as r_s for the shooter.

Algorithm 1 outlines the termination procedure that is incorporated at each time step in our simulations. It involves a simple loop through all the individuals during the entire simulation period T. The simulation calculates the distance between each individual and the shooter. If the distance falls below the specified shot radius r_s and the individual is outside the safe zone Z_s, the targeted individual is eliminated from the simulation. The total number of individuals, N, is then decreased accordingly, and the number of casualties, K, will increase by 1. The output of this algorithm includes the final number of casualties, denoted by K, and the set of survived individuals, represented by $\mathcal{V}_s$. These individuals will be included in the dynamic simulations for the next time step. It is assumed that the shooter is not able to harm the guiding agent, even if the guiding agent is within the shot radius of the shooter.

Algorithm 1: Termination Procedure

Input: $\mathbf{x}_j$, $\mathbf{z}$, N, K, r_s, Z_s
Output: K, $\mathcal{V}_s$

```
for j ← 1 to N do
    d = |x_j − z|;
    if d < r_s and x_j ∉ Z_s then
        remove j from V;
        N ← N − 1;
        K ← K + 1;
```

C. Impact of Individual Behaviors on the Outcomes of Mass Shooting Scenarios

In the study of crowd dynamics and mass shooting scenarios, it is crucial to recognize the impact of individual behaviors, including the individuals and the guiding agent, on the overall outcome. When individuals exhibit a high attraction strength ($\alpha_1 > 0$) and tend to cluster together, it can potentially facilitate the shooter in causing more casualties. Conversely, intentional distancing among individuals (low attraction strength or repulsive interaction with $\alpha_1 < 0$) tends to decrease the initial number of casualties by making it more challenging for the shooter to target dispersed individuals. However, while individuals may strive to become more dispersed to minimize the shooter's impact, excessive dispersal, e.g., highly negative α_1, can lead to challenges in following the directions of the guiding agent. This could result in unintended consequences, as it becomes easier for the shooter to track and inflict harm on individuals over time.

Additionally, the approach taken by the guiding agent, represented by the parameter λ in our model, is another crucial factor in determining escape outcomes. Simply focusing on reaching the safe zone may not always result in minimizing the severity of the situation. Similarly, moving away from the shooter at the expense of guiding individuals far from the safe zone is not desirable.

The correlation between the number of casualties (K), the attraction/repulsion strength (α_1), and the guiding agent's decisions (λ) can be observed in Fig. 1. This figure highlights the influence of individual behaviors on the outcomes of

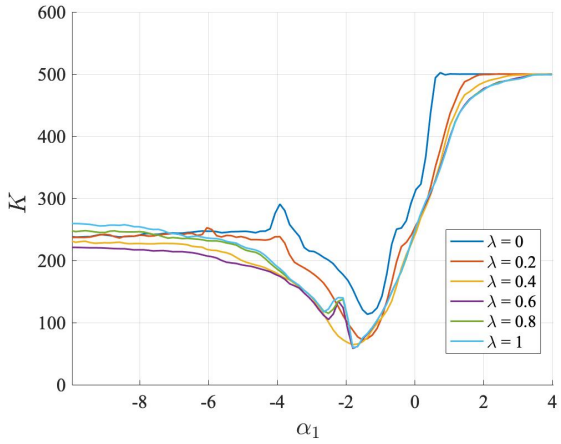

Fig. 1: The impact of attraction/repulsion strength (α_1) on the average number of casualties for varying values of λ in a crowd with $N = 500$. The average number of casualties is obtained by averaging over five iterations, each utilizing random initial positions for the crowd members.

the scenario. The crowd consists of $N = 500$ individuals whose initial positions in the room, are randomly distributed. The shooter and the guiding agent are initially located at $\mathbf{z}_0 = [3, 1]$ and $\mathbf{y}_0 = [0.8, 0.8]$, respectively. The simulation is conducted with the following parameter values: $\alpha_2 = 0.2$, $\alpha_3 = -1$, $\alpha_4 = 5$, $\alpha_5 = 5$, $\alpha_6 = 0.1$, $p = 2.5$, $r_s = 0.4$, $r_w = 0.5$, $T = 10$, $\mathbf{y}_r = [3.75, 3.75]$.

The observations from Fig. 1 highlight the existence of a critical threshold for both individuals and guiding agent actions. Specifically, in this scenario, when crowd members exhibit extreme behaviors, such as closely following others ($\alpha_1 \to 4$) or attempting to move away from individuals ($\alpha_1 \to -10$), the effectiveness of the guiding agent diminishes. Conversely, the guiding agent emerges as a crucial factor in minimizing casualties when the crowd demonstrates rational movements – balancing between following others and avoiding tightly packed groups. Therefore, cooperation between the crowd and the guiding agent may result in fewer casualties. Building upon this observation, the subsequent section focuses on designing an effective escape policy that involves the active participation and cooperation of both individuals and the guiding agent.

III. Optimizing Guidance and Crowd Movement toward Safe Zone

In scenarios where a large crowd is confined to a room and under attack by a shooter, the exposure to the shooter and, consequently, the number of casualties are significantly influenced by two key factors:

- Proximity to the shooter: The exposure increases if, on its way to the safe zone, the guiding agent moves closer to the shooter, i.e., $\lambda \to 1$, as this brings the individuals in closer proximity to the shooter as well.
- Formation of large clusters, i.e., large α_1: The exposure also increases if the individuals tend to cluster together in a tight formation. Large clusters are more easily accessible to the shooter, posing a higher risk to the individuals.

By carefully considering the impact of both the guiding agent's decisions, reflected on parameter λ, and the individuals' reactions, reflected on parameter α_1, we can design strategies that optimize the escape scenario toward the safe zone. To accomplish this, we present an optimization problem based on the movement of the guiding agent and the individuals. The objective is to minimize the number of casualties K during the escape process toward the safe zone while avoiding the shooter.

The following optimization problem is designed to tune the evacuation factors α_1 and λ in order to minimize the number of casualties K in a given crowd during an evacuation process over a specified time interval T.

$$\begin{aligned} \underset{\alpha_1,\lambda}{\text{minimize}} \quad & K = \sum_{t=1}^{T}\sum_{j=1}^{N} I(|\mathbf{x}_j(t) - \mathbf{z}(t)| < r_s) \\ \text{subject to} \quad & \mathbf{x}(0) = \mathbf{x}_0,\ \mathbf{z}(0) = \mathbf{z}_0,\ \mathbf{y}(0) = \mathbf{y}_0, \\ & (2),\ (3),\ (4), \\ & 0 \le \lambda \le 1, \end{aligned} \tag{5}$$

where

$$I(|\mathbf{x}_j(t) - \mathbf{z}(t)| < r_s) = \begin{cases} 1 & \text{if} \quad |\mathbf{x}_j(t) - \mathbf{z}(t)| < r_s, \\ 0 & \text{otherwise.} \end{cases} \tag{6}$$

The objective function K represents the total number of casualties, which is obtained by summing up the indicator functions for all the individuals and time intervals.

In what follows, we present two simulated shooting scenarios using the dynamics from Section II in the specified environment. The simulated crowd consists of $N = 500$ individuals initially scattered randomly in the danger zone, shown as blue dots in Fig. 2a. The shooter is denoted by $\times$, and the guiding agent by $+$. We maintain the same parameters as in Fig. 1 for all simulations. Note that if the crowd jams against the walls, individuals may exert a force against the wall to free themselves and move toward the safe zone.

In the initial scenario, as depicted in Figs. 2b, 2c, and 2d, the individuals demonstrate a strong tendency to cluster together due to the influence of an interaction strength parameter of $\alpha_1 = 1$. This leads to the formation of a tightly grouped crowd. On the other hand, the guiding agent's priority lies in distancing itself from the shooter to minimize the risk to the crowd, indicated by a low value of $\lambda = 0.1$. Once the guiding agent reaches the safe zone, it maintains its position at the designated target to ensure the crowd's safety.

In an attempt to pursue the crowd, the shooter advances until reaching the boundaries of the safe zone, where they are ultimately captured, marking the termination of the scenario. The combination of crowd clustering and the guiding agent's movement leads to a significant casualty count of $K = 450$.

To avoid outcomes such as the one represented in Figs. 2, we have employed the optimization algorithm presented in (5) and used the Bayesian Optimization toolbox in Matlab

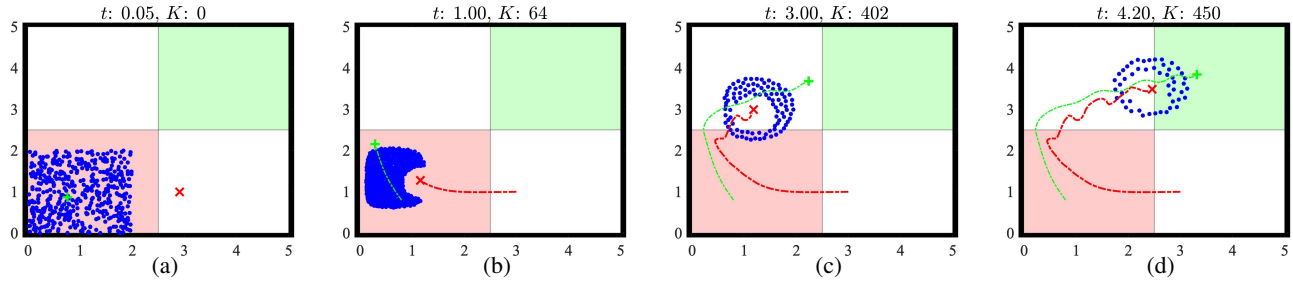

Fig. 2: A composite figure illustrating three distinct stages of a simulated crowd guidance scenario for $N = 500$ with parameter values $\alpha_1 = 1$ and $\lambda = 0.1$. The blue dots represent the individuals, the symbol $\times$ indicates the shooter, and the symbol $+$ represents the guiding agent.

[22] to determine the optimal values of parameters α_1 and λ to minimize the number of casualties, denoted as K. Through the optimization process conducted for 10 iterations with different random initial positions for individuals, an average of observed minimum casualties $\bar{K}^* = 69.6$ for the average optimal values of $\bar{\alpha}_1 = -1.6250$ and $\bar{\lambda} = 0.7135$ was achieved. [1]

IV. Equilibrium

In this section, we study the equilibrium configuration of the crowd with respect to the positions of the shooter and the guiding agent, as well as the escape parameters. To conduct an equilibrium analysis of the system described by equations (2)-(4), we assume that all interactions occur within an open environment ($\alpha_6 = 0$), and that both the shooter and guiding agent have attained a stationary state, implying $\frac{\mathrm{d}\mathbf{z}}{\mathrm{d}t} = 0$ and $\frac{\mathrm{d}\mathbf{y}}{\mathrm{d}t} = 0$. This assumption is considered valid for the scope of our analysis, which focuses on the equilibrium states of the system. Namely, equilibrium in this context refers to the state of the system when time goes to infinity, during which the guiding agent has established its position within the safe zone. In parallel, the shooter has reached a decisive moment—either being captured at the boundary of the safe zone or being encircled by the crowd, thereby unable to decide its path due to the symmetry of the crowd. This effectively confirms the assumed velocities for both the shooter and the guiding agent. Additionally, we assume that at equilibrium, the crowd will aggregate with individuals maintaining a relatively close distance, i.e., $|\mathbf{x}_j - \mathbf{x}_k| < r_0$ for all $j, k \in \mathcal{V}$, which implies $h(r) = 1$. The subsequent simulation results confirm the validity of this assumption.

Leveraging the analytical advantages offered by the continuum models [24], we subsequently proceed to establish the continuum-limit model for the crowd as described by equation (2), while taking into account the aforementioned assumptions. In the continuum-limit model, we consider the number of individuals to be infinite. This assumption accommodates the mean-field approximation of the crowd, introducing a new perspective to the problem. The expectation is that the outcomes derived from the discrete model will be consistent with those obtained from the continuum-limit model, as the continuum model essentially represents a mean-field approximation of its discrete counterpart [25]. As the number of individuals N approaches infinity, the dynamics of the crowd convergese to the following continuum model.

$$\frac{\partial \rho(\mathbf{x},t)}{\partial t} + \nabla \cdot (\rho(\mathbf{x},t)\mathbf{v}(\mathbf{x},t)) = 0, \tag{7}$$

$$\mathbf{v}(\mathbf{x},t) = \int_{\mathbb{R}^2} \left(\frac{\mathbf{x}-\mathbf{w}}{|\mathbf{x}-\mathbf{w}|^2} - \alpha_1(\mathbf{x}-\mathbf{w}) \right) \rho(\mathbf{w},t)\mathrm{d}\mathbf{w} + \alpha_2 \frac{\mathbf{x}-\mathbf{z}}{|\mathbf{x}-\mathbf{z}|^2} + \alpha_3(\mathbf{x}-\mathbf{y}). \tag{8}$$

Here, $\rho(\mathbf{x},t) \in \mathbb{R}$ denotes the density distribution of the crowd at position $\mathbf{x}$ and time t, satisfying $\int_{\mathbb{R}^2} \rho(\mathbf{w},t)\mathrm{d}\mathbf{w} = 1$. The velocity field of the crowd is represented by $\mathbf{v}(\mathbf{x},t)$. Initially, the crowd is distributed with a density probability distribution of $\rho(\mathbf{x},0) = \frac{1}{N}\sum_{j=1}^{N} \delta(\mathbf{x}-\mathbf{x}_j)$, where δ is the delta function. The assumption of a small shot radius ($r_s \to 0$) ensures the conservation of mass in the crowd, as described by (7).

The following theorem outlines an equilibrium configuration of the crowd. The analytical approach adopted in this section closely follows that of [16]. However, the inclusion of a guiding agent in our analysis has led to a generalization of the crowd's equilibrium configuration for different scenarios.

Theorem 1: Consider a crowd with dynamics (7) and (8), where both the shooter and the guiding agent are stationary. If the distance between the shooter and guiding agent satisfies $|\mathbf{z}-\mathbf{y}| \le d_1$ (refer to Table I(D)), then the the dynamics admit an equilibrium state in which individuals uniformly distribute within the region $\mathcal{A} = \{\mathbf{x} \mid |\mathbf{x}-\mathbf{c}_1| \ge R_1, |\mathbf{x}-\mathbf{c}_2| \le R_2\}$, where

$$d_1 = \frac{\alpha_3}{\alpha_1\alpha_2+\alpha_3}(R_2-R_1),$$
$$R_1 = \sqrt{\frac{\alpha_2}{\alpha_1-\alpha_3}}, \quad \mathbf{c}_1 = \mathbf{z},$$
$$R_2 = \sqrt{\frac{1+\alpha_2}{\alpha_1-\alpha_3}}, \quad \mathbf{c}_2 = \frac{\alpha_1\alpha_2\mathbf{z}+\alpha_3\mathbf{y}}{\alpha_1\alpha_2+\alpha_3}.$$

Proof: Define characteristic curves $\mathbf{X}(\mathbf{X}_0,t)$ such that for $\mathbf{x} = \mathbf{X}(\mathbf{X}_0,t)$ we have $\frac{\mathrm{d}\mathbf{x}}{\mathrm{d}t} = \mathbf{v}(\mathbf{x},t)$ and a constant density distribution $\rho(\mathbf{x},t)$ along $\mathbf{X}$, which is a valid assumption based on [26]. Specifically, since the nonlinearities

[1]The simulated evacuation scenarios described in this paper, as well as the associated MATLAB code, can be accessed via the GitHub repository provided in [23].

(A). No shooter or guiding agent ($\alpha_2, \alpha_3 = 0$)	(B). Shooter only ($\alpha_3 = 0$)	(C). Guiding agent only ($\alpha_2 = 0$)	(D). $\lvert\mathbf{z}-\mathbf{y}\rvert \le d_1$	(E). $d_1 < \lvert\mathbf{z}-\mathbf{y}\rvert < d_2$	(F). $\lvert\mathbf{z}-\mathbf{y}\rvert \ge d_2$
$R = \sqrt{\frac{1}{\alpha_1}}$ $\mathbf{c} = \bar{\mathbf{x}}$	$R_1 = \sqrt{\frac{\alpha_2}{\alpha_1}}$ $R_2 = \sqrt{\frac{1+\alpha_2}{\alpha_1}}$ $\mathbf{c}_1 = \mathbf{c}_2 = \mathbf{z}$	$R = \sqrt{\frac{1}{\alpha_1-\alpha_3}}$ $\mathbf{c} = \mathbf{y}$	$R_1 = \sqrt{\frac{\alpha_2}{\alpha_1-\alpha_3}}$ $\mathbf{c}_1 = \mathbf{z}$ $R_2 = \sqrt{\frac{1+\alpha_2}{\alpha_1-\alpha_3}}$ $\mathbf{c}_2 = \frac{\alpha_1\alpha_2\mathbf{z}+\alpha_3\mathbf{y}}{\alpha_1\alpha_2+\alpha_3}$	$R_1 \approx \sqrt{\frac{\alpha_2}{\alpha_1-\alpha_3}}$ $\mathbf{c}_1 \approx \mathbf{z}$ $R_2 \approx \sqrt{\frac{1+\alpha_2}{\alpha_1-\alpha_3}}$ $\mathbf{c}_2 \approx \frac{\alpha_1\alpha_2\mathbf{z}+\alpha_3\mathbf{y}}{\alpha_1\alpha_2+\alpha_3}$	$R = \sqrt{\frac{1}{\alpha_1-\alpha_3}}$ $\mathbf{c} = \mathbf{y}$
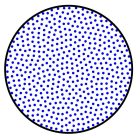	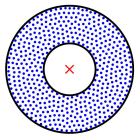	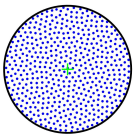	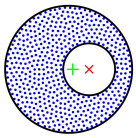	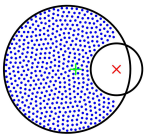	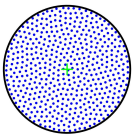

TABLE I: Equilibrium configuration of the crowd depending on the presence of the shooter and the guiding agent and their distance at equilibrium. The blue dots, symbol $\times$, and symbol $+$ represent the individuals, shooter, and guiding agent, respectively. Solid circles correspond to the continuum-limit asymptotics. The figures are generated using parameters $\alpha_1 = 1$, $\alpha_2 = \{0, 0.2\}$, and $\alpha_3 = \{0, -1\}$ depending on the presence of the shooter and guiding agent.

in (2) are deliberately chosen to be Newtonian, the density remains constant inside the swarm. As a result, the mass conservation equation (7) along the characteristic curves is simplified to

$$\frac{\mathrm{d}\rho}{\mathrm{d}t} = -\left(\nabla_{\mathbf{x}} \cdot \mathbf{v}\right)\rho. \tag{9}$$

We next obtain the divergent of crowd's velocity field for $\mathbf{x} \neq \mathbf{z}$ and $\mathbf{x} \neq \mathbf{y}$. Using the identity $\nabla_x \cdot (\frac{\mathbf{x}-\mathbf{z}}{|\mathbf{x}-\mathbf{z}|^2}) = \Delta_x(\ln|\mathbf{x}-\mathbf{z}|) = 2\pi\delta(\mathbf{x}-\mathbf{z})$, (8) yields

$$\nabla_{\mathbf{x}} \cdot \mathbf{v} = 2\pi\rho - 2\alpha_1 + 2\alpha_3, \tag{10}$$

which returns the following solution to the ordinary differential equation (9)

$$\rho(t) = \frac{(\alpha_1-\alpha_3)\rho_0 e^{2t(\alpha_1-\alpha_3)}}{\pi(\rho_0 e^{2t(\alpha_1-\alpha_3)} - 1) + \alpha_1 - \alpha_3}, \tag{11}$$

where $\rho_0 = \rho\left(\mathbf{X}_0, 0\right)$. Note that obtaining the crowd density solely as a function of time directly stems from the assumption of constant density field along characteristic curves.

As (11) suggests, for any $\rho_0 > 0$ and $\alpha_1 - \alpha_3 > 0$, the crowd density distribution will approach $\lim_{t\to\infty}\rho(t) = \frac{\alpha_1-\alpha_3}{\pi}$. It is worth noting that when $\alpha_1 - \alpha_3 < 0$, we observe $\lim_{t\to\infty}\rho(t) = 0$, signifying that the repulsion interaction among individuals surpasses their attraction towards the guiding agent, leading to dispersion of the crowd and the density approaching zero in the continuum.

We now aim to identify a steady state in which the crowd has reached a stationary condition, meaning $\mathbf{v}(\mathbf{x}, t) = 0$. We seek a steady state in which the crowd aggregate inside an off-center annular area described by $\mathcal{A} = \{\mathbf{x} \mid |\mathbf{x}-\mathbf{c}_1| \ge R_1, |\mathbf{x}-\mathbf{c}_2| \le R_2\}$ where $\mathbf{c}_1 = \mathbf{z}$ and $|\mathbf{z}-\mathbf{y}| \le d_1$. Using (8), we can determine the velocity field of the crowd along the characteristic curves $\mathbf{x} = \mathbf{X}\left(\mathbf{X}_0, t\right)$ within $\mathcal{A}$ as follows

$$\mathbf{v}(\mathbf{x},t) = \rho\pi(\mathbf{x}-\mathbf{c}_2) - \rho\pi R_1^2\frac{\mathbf{x}-\mathbf{z}}{|\mathbf{x}-\mathbf{z}|^2} + \alpha_1\bar{\mathbf{x}} - \rho\pi\alpha_1\mathbf{x}\left(R_2^2 - R_1^2\right) + \alpha_2\frac{\mathbf{x}-\mathbf{z}}{|\mathbf{x}-\mathbf{z}|^2} + \alpha_3(\mathbf{x}-\mathbf{y}). \tag{12}$$

This expression is obtained using the following identity for both areas indicated by $|\mathbf{x}-\mathbf{c}_1| \ge R_1$ and $|\mathbf{x}-\mathbf{c}_2| \le R_2$, while shifting the origin with respect to the corresponding center of these circles.

$$\int_{|\mathbf{w}|\le R}\frac{\mathbf{x}-\mathbf{w}}{|\mathbf{x}-\mathbf{w}|^2}\,\mathrm{d}\mathbf{w} = \begin{cases}\pi R^2\frac{\mathbf{x}}{|\mathbf{x}|^2} & |\mathbf{x}| > R,\\ \pi\mathbf{x} & |\mathbf{x}| < R.\end{cases} \tag{13}$$

By replacing $\bar{\mathbf{x}}$ in (12) using the simple geometry rule $\mathbf{c}_2R_2^2 = \bar{\mathbf{x}}(R_2^2 - R_1^2) + \mathbf{z}R_1^2$ as well as replacing the steady state density by $\lim_{t\to\infty}\rho(t) = \frac{\alpha_1-\alpha_3}{\pi}$, we get

$$\mathbf{v}(\mathbf{x},t) = (\alpha_1-\alpha_3)(\mathbf{x}-\mathbf{c}_2) - (\alpha_1-\alpha_3)R_1^2\frac{\mathbf{x}-\mathbf{z}}{|\mathbf{x}-\mathbf{z}|^2} + \alpha_1\frac{\mathbf{c}_2R_2^2 - \mathbf{z}R_1^2}{R_2^2-R_1^2} - \alpha_1(\alpha_1-\alpha_3)(R_2^2-R_1^2)\mathbf{x} + \alpha_2\frac{\mathbf{x}-\mathbf{z}}{|\mathbf{x}-\mathbf{z}|^2} + \alpha_3(\mathbf{x}-\mathbf{y}). \tag{14}$$

A proof follows by solving the equation (14) for R_1, R_2 and $\mathbf{c}_2$ such that zero velocity for all $\mathbf{x} \in \mathcal{A}$ is guaranteed. The three following equations are derived from setting the vector field $\mathbf{v}(\mathbf{x}, t)$ to zero.

$$\left[\frac{(\alpha_1-\alpha_3)R_1^2}{|\mathbf{x}-\mathbf{z}|^2} + \frac{\alpha_2}{|\mathbf{x}-\mathbf{z}|^2}\right](\mathbf{x}-\mathbf{z}) = \mathbf{0}, \tag{15a}$$

$$\left[(\alpha_1-\alpha_3) - \alpha_1(\alpha_1-\alpha_3)(R_2^2-R_1^2) + \alpha_3\right]\mathbf{x} = \mathbf{0}, \tag{15b}$$

$$-(\alpha_1-\alpha_3)\mathbf{c}_2 + \alpha_1\frac{\mathbf{c}_2R_2^2 - \mathbf{z}R_1^2}{R_2^2-R_1^2} - \alpha_3\mathbf{y} = \mathbf{0}. \tag{15c}$$

From (15a), (15b), and (15c), we deduce $R_1 = \sqrt{\frac{\alpha_2}{\alpha_1-\alpha_3}}$, $R_2 = \sqrt{\frac{1+\alpha_2}{\alpha_1-\alpha_3}}$, and $\mathbf{c}_2 = \frac{\alpha_1\alpha_2\mathbf{z}+\alpha_3\mathbf{y}}{\alpha_1\alpha_2+\alpha_3}$ respectively. ■

The same analytical approach can be taken to determine the precise equilibrium configuration of the crowd for the scenarios represented in Table I(A), (B), (C), and (F), where $d_2 = \frac{\alpha_3}{\alpha_1\alpha_2+\alpha_3}(R_2+R_1)$.

When the shooter and guiding agent are within $d_1 < |\mathbf{z} - \mathbf{y}| < d_2$ (Table I(E)), the approximate crowd configuration can be obtained using the same parameters R_1, R_2, $\mathbf{c}_1$, and $\mathbf{c}_2$ as in case $|\mathbf{z} - \mathbf{y}| \leq d_1$. However, as the distance between the shooter and the guiding agent increases, this approximation becomes less accurate. It is also worth noting that for the case with no guiding agent (Table I(B)), the shooter is assumed free to move and follow the crowd. By the time $t \to \infty$, this interaction leads to a static state for both shooter and the individuals, attributed to the crowd symmetrically surrounding the shooter who is stabilizing its position. Consequently, the crowd formation follows Theorem 1 and the proof outlined earlier in this section. This observation explains the convergence of the crowd to a circular formation that envelopes the shooter. When the shooter is in a stationary state and there is no guiding agent in the vicinity, the configuration in case (A) of the table is observed, where individuals form a circle away and out of the influence of the shooter as if the shooter's presence is ineffective ($\alpha_2 = 0$). Overall, as Table I demonstrates, the discrete model's outcomes (visualized as blue dots) are in agreement with the continuum model's equilibrium prediction (illustrated by solid circles).

Acknowledgements: The authors would like to thank Dr. Jared Miller for his valuable comments.

V. Conclusion

In this study, we propose a hybrid approach for dynamical modeling and guiding crowds in mass shooting scenarios. The presented PSG model relies on pairwise repulsive and attractive interactions among individuals to predict their movement while considering a given set of evacuation factors. These factors define both the psychological and physical parameters of such events. The observations derived from our PSG model suggest that in scenarios where individuals within a crowd exhibit erratic behaviors, such as excessive aggregation or dispersion, it becomes increasingly challenging for the guiding agent to exert effective control over their movements, highlighting the crucial role of cooperation between the crowd and guiding agent for a secure escape to a safe zone. Through our model, we have developed an optimized motion strategy for both the guiding agent and the crowd, aiming to minimize casualties in specific scenarios. Furthermore, the steady-state analysis provides valuable insights into crowd configurations based on evacuation parameters and the positions of the shooter and guiding agent. Future research can enhance the PSG model by considering factors like reaction times and familiarity with building layouts.

References

[1] J. J. Fruin, "The causes and prevention of crowd disasters," *Engineering for crowd safety*, vol. 1, no. 10, pp. 99–108, 1993.

[2] A. A. Khan and E. K. Noji, "Hajj stampede disaster, 2015: Reflections from the frontlines.," *American journal of disaster medicine*, vol. 11, no. 1, pp. 59–68, 2016.

[3] D. Helbing, A. Johansson, and H. Z. Al-Abideen, "Dynamics of crowd disasters: An empirical study," *Physical review E*, vol. 75, no. 4, p. 046109, 2007.

[4] A. Sharma, B. McCloskey, D. S. Hui, A. Rambia, A. Zumla, T. Traore, S. Shafi, S. A. El-Kafrawy, E. I. Azhar, A. Zumla, *et al.*, "Global mass gathering events and deaths due to crowd surge, stampedes, crush and physical injuries-lessons from the seoul halloween and other disasters," *Travel medicine and infectious disease*, vol. 52, 2023.

[5] "Gun violence archive," June 16, 2023. June 16, 2023.

[6] D. J. Sumpter, R. P. Mann, and A. Perna, "The modelling cycle for collective animal behaviour," *Interface focus*, vol. 2, no. 6, pp. 764–773, 2012.

[7] D. Helbing and P. Molnar, "Social force model for pedestrian dynamics," *Physical review E*, vol. 51, no. 5, p. 4282, 1995.

[8] T. Vicsek, A. Czirók, E. Ben-Jacob, I. Cohen, and O. Shochet, "Novel type of phase transition in a system of self-driven particles," *Physical review letters*, vol. 75, no. 6, p. 1226, 1995.

[9] A. Czirók and T. Vicsek, "Collective behavior of interacting self-propelled particles," *Physica A: Statistical Mechanics and its Applications*, vol. 281, no. 1-4, pp. 17–29, 2000.

[10] R. L. Hughes, "A continuum theory for the flow of pedestrians," *Transportation Research Part B: Methodological*, vol. 36, no. 6, pp. 507–535, 2002.

[11] D. C. Duives and H. S. Mahmassani, "Exit choice decisions during pedestrian evacuations of buildings," *Transportation Research Record*, vol. 2316, no. 1, pp. 84–94, 2012.

[12] S. Gunn, P. B. Luh, X. Lu, and B. Hotaling, "Optimizing guidance for an active shooter event," in *2017 IEEE International Conference on Robotics and Automation (ICRA)*, pp. 4299–4304, IEEE, 2017.

[13] X. Lu, P. B. Luh, K. L. Marsh, T. Gifford, and A. Tucker, "Guidance optimization of building evacuation considering psychological features in route choice," in *Proceeding of the 11th World Congress on Intelligent Control and Automation*, pp. 2669–2674, IEEE, 2014.

[14] M. Xu, X. Xie, P. Lv, J. Niu, H. Wang, C. Li, R. Zhu, Z. Deng, and B. Zhou, "Crowd behavior simulation with emotional contagion in unexpected multihazard situations," *IEEE Transactions on Systems, Man, and Cybernetics: Systems*, vol. 51, no. 3, pp. 1567–1581, 2021.

[15] Z. Tian, G. Zhang, H. Yu, H. Liu, and D. Lu, "Negemotion: Explore the double-edged sword effect of negative emotion on crowd evacuation," *IEEE Transactions on Computational Social Systems*, pp. 1–14, 2024.

[16] Y. Chen and T. Kolokolnikov, "A minimal model of predator–swarm interactions," *Journal of The Royal Society Interface*, vol. 11, no. 94, p. 20131208, 2014.

[17] M. Zhou, H. Dong, P. A. Ioannou, Y. Zhao, and F.-Y. Wang, "Guided crowd evacuation: approaches and challenges," *IEEE/CAA Journal of Automatica Sinica*, vol. 6, no. 5, pp. 1081–1094, 2019.

[18] M. Bongini and G. Buttazzo, "Optimal control problems in transport dynamics," *Mathematical Models and Methods in Applied Sciences*, vol. 27, no. 03, pp. 427–451, 2017.

[19] H. Tomkins and T. Kolokolnikov, "Swarm shape and its dynamics in a predator-swarm model," *preprint*, 2014.

[20] M. Moussaïd, N. Perozo, S. Garnier, D. Helbing, and G. Theraulaz, "The walking behaviour of pedestrian social groups and its impact on crowd dynamics," *PloS one*, vol. 5, no. 4, p. e10047, 2010.

[21] L. Bruno and A. Corbetta, "Uncertainties in crowd dynamic loading of footbridges: A novel multi-scale model of pedestrian traffic," *Engineering structures*, vol. 147, pp. 545–566, 2017.

[22] "Matlab bayesian optimization toolbox." `https://www.mathworks.com/help/stats/bayesopt.html`, 2023.

[23] "PSG Model." `https://github.com/SiamiLab/PSGModel`, 2023.

[24] A. J. Bernoff and C. M. Topaz, "A primer of swarm equilibria," *SIAM Journal on Applied Dynamical Systems*, vol. 10, no. 1, pp. 212–250, 2011.

[25] J.-Y. L. Boudec, D. McDonald, and J. Mundinger, "A generic mean field convergence result for systems of interacting objects," in *Fourth International Conference on the Quantitative Evaluation of Systems (QEST 2007)*, pp. 3–18, 2007.

[26] R. C. Fetecau, Y. Huang, and T. Kolokolnikov, "Swarm dynamics and equilibria for a nonlocal aggregation model," *Nonlinearity*, vol. 24, no. 10, p. 2681, 2011.